Supporting Information

Dual-confinement Strategy to Construct Cobalt based Phosphides Nanocluster within Carbon Nanofiber for Bifunctional Water Splitting Electrocatalyst

Jie Chen,[a,b,*] Fuying Huang,[a,b] Sunzai Ke,[a] Jiaxin Shen,[a] Yancai Li,[a,b] Fengying Zheng,[a,b] Shunxing Li[a,b,*]

a College of Chemistry, Chemical Engineering and Environment, Minnan Normal University, Zhangzhou, 363000, China.
b Fujian Province Key Laboratory of Modern Analytical Science and Separation Technology, Minnan Normal University, Zhangzhou, 363000, China

E-mail: chenj@mnnu.edu.cn; shunxing_li@aliyun.com; Fax: +86-596-2591395; Tel: +86-596-2591395.

Experimental

Reagents and chemicals

Polyacrylonitrile (PAN, Mw = 150,000) and Nafion solution was purchased from Sigma-Aldrich Co. Ltd. 2-Methylimidazole (MeIM), cobalt nitrate hexahydrate ($Co(NO_3)_2 \cdot 6H_2O$), nickel (II) acetylacetonate ($Ni(acac)_2$) and copper (II) acetylacetonate ($Cu(acac)_2$) were purchased from Aladdin. N, N-dimethylformamide (DMF) and sodium hypophosphite (NaH_2PO_2) were purchased from Shantou Xilong Chemical Industry Incorporated Co., Ltd. Commercial Pt/C (20 wt% Pt on Vulcan XC72) and RuO_2 catalyst were purchased from Sigma-Aldrich Chemical Reagent Co., Ltd. All the reagents have reached the degree of analytical reagent. Ultrapure water (Millipore Milli-Q grade) with a resistivity of 18.2 MΩ was used in all the experiments.

Synthesis of ZIF-67

In a typical preparation, 0.45 g $Co(NO_3)_2 \cdot 6H_2O$ was dissolved in 3 mL of water, then 5.5 g MeIM was dissolved in 20 mL of water. Those two solutions were mixed (Co^{2+} : MeIM : H_2O = 1 : 58 : 1100) and stirred for 6 h at room temperature, then the resulting purple precipitates were collected by centrifuging, washed with water and methanol subsequently for 3 times, and finally vacuum dried at 80 ℃ for 24 h.

Synthesis of Ni-ZIF-67 and Cu-ZIF-67

In a typical synthesis, 100 mg ZIF-67 powders were mixed with 50 ml

ethanol by ultra-sonification for 30 min to form a homogeneous dispersion.

20 mg $Ni(acac)_2$ or $Cu(acac)_2$ were then added into the dispersion, with rigorously stirring until the ethanol evaporated out, forming Ni-ZIF-67 and Cu-ZIF-67 mixtures, respectively. The mixture was finally vacuum dried at 80 ℃ for 24 h.

Synthesis of ZIF-PAN fiber

PAN and ZIF-67 were adopted as the carbon and cobalt precursors, respectively, and DMF was chosen as the solvent. First, 0.1 g ZIF-67 was added to 5 ml DMF and stirred for 2 h to form a homogenous solution. Then, 0.5 g PAN was added into the solution and stirred for 2h in a water bath at 80 ℃. The as-prepared precursor solution was transferred into a 10 ml syringe with a needle (outer diameter = 0.7mm). An electrospinning unit (Lvna Tech. Co., China) with a high voltage of 13.5 kV was applied, and a constant distance of 15 cm was regulated between the needle and rotation collector. The electrospun composite was collected on an aluminum foil in the collector with a flow rate of 2 ml h^{-1}. The composite was then peeled off from the collector and stabilized at 60 ℃ for overnight in a vacuum oven. The as-synthesized ZIF-PAN fiber was placed at the middle of a porcelain boat and NaH_2PO_2 (mass ratio 1:10) was placed at the upstream side. The porcelain boat was put in a tube furnace and heated to 350 °C with a ramp rate of 2 °C·min^{-1} and kept for 2 h. Then the ZIF-

PAN fiber was carbonized at 700 ℃ for another 2 h under nitrogen atmosphere with a heating rate of 5 ℃ min^{-1}. The final product was named CoP_x-CNFs. For comparison, ZIF-67 was also treated using the same process and named CoP_x-CPHs. Similarly, the bimetallic $CoNiP_x$ and $CoCuP_x$ samples were prepared using the Ni-ZIF-67 and Cu-ZIF-67 as the precursors.

Materials characterization

The morphology and microstructure of the catalysts were characterized by scanning electron microscopy (SEM, Hitachi S-4800), transmission electron microscopy (TEM, FEI Tecnai G20) and high-resolution transmission electron microscopy (HRTEM, FEI Tecnai F20) operated at 200 kV. Powder X-ray diffraction (XRD) patterns were collected on a Rigaku D/max 2500 diffract meter with Cu K radiation (λ=1.54056 Å). The Co, Ni and Cu contents of above samples were determined by ICP-MS (PerkinElmer NexION 300X), and the C, N, P contents were analyzed by CHN elemental analysis (Vario MACRO). The X-ray photoelectron spectroscopy (XPS) were performed by an ESCALAB 250 Xi XPS system of Thermo Scientific, where the analysis chamber was 1.5×10^{-9} mbar and the X-ray spot was 500 nm.

Electrochemical measurements

The electrochemical measurements were carried on an electrochemical workstation (CHI 660E, CH Instruments, Shanghai) using a three-electrode

analysis system. For the preparation of the working electrode, 4 mg CoP_x-CPHs was dispersed in 1 mL DMF by sonication (To ensure the same amount of active substance, the loading of CoP_x-CNFs was 20 mg), then 20 μL of 5 wt% Nafion solution was added until a homogeneous suspension formed. Next, 10 μL of the above suspension was drop-casted onto a glassy carbon electrode (d = 3 mm, S = 0.07065 cm^2) to give a mass loading of about 0.5 mg cm^{-2}. An Ag/AgCl (0.3 M KCl) electrode was used as the reference electrode and graphite rod as the counter electrode. The potential measured against an Ag/AgCl electrode was converted to the potential versus the reversible hydrogen electrode (RHE) according the formulation: E (vs. RHE) = E (vs. Ag/AgCl) + 0.059 × pH + 0.210. Linear sweep voltammetry (LSV) polarization curves for HER and OER were both carried out with a scan rate of 10 mV s^{-1} in N_2-saturated condition, and all the polarization curves were without iR-correction. EIS was performed at open circuit potential and 200 mV overpotential within the frequency range of 0.1 to 100 kHz and an a.c. voltage of 10 mV. Because of the less content of the second metal, the loading of bimetallic $CoNiP_x$ and $CoCuP_x$ samples were the same as CoP_x samples (4 mg for $CoNiP_x$ and $CoCuP_x$ CPHs, 20 mg for $CoNiP_x$ and $CoCuP_x$ CNFs). A two-electrode water electrolyze device was assembled using CoNiPx-CNFs paper (1 × 2 cm) prepared from the ZIF-PAN film after the phosphidation and carbonization treatment as a bifunctional electrocatalyst for both OER and

HER. The loading mass of this self-supported $CoNiP_x$-CNFs electrode was 10 mg cm^{-2}. The electrocatalytic activity was examined by measuring the LSV curve in 1.0 M KOH solution with a scan rate of 10 mV s^{-1}.

To prepare Pt/C and RuO_2 electrode, 4 mg Pt/C or RuO_2 powder and 20 μL 5 wt% Nafion solution were dispersed in 1 mL DMF solvent by 30 min sonication to form an ink. Then 10 μL catalyst ink was loaded on glassy carbon electrode and air-dried at room temperature.

The faradaic efficiency was calculated using the formula $\eta = n(gas)_{generation}/n(gas)_{theory}$. The hydrogen and oxygen generated from cathode and anode could be collected and measured in 1 h of durability test at current density of 10 mA cm^{-2}. The theoretical O_2 yields were calculated as follows: $n(O_2) = Q/(nF)$, where $n(O_2)$ is the number of moles of oxygen produced, Q is the charge passed through the electrodes, F is the Faradaic constant (96485 C mol^{-1}), and n is the number of electrons transferred during water splitting (4 mol of electrons per mole of O_2); the theoretical H_2 yields were calculated in the same way as O_2 yields except 4 mol of electrons were transferred per 2 mol of H_2.

The turnover frequency (TOF) of $CoNiP_x$-CNFs electrocatalyst was calculated according to the following equation: $TOF = j \times S/(4 \times F \times n)$, where j is the current density obtained at overpotential of 300 mV, S is the surface area of the electrode, F is the Faraday efficiency (96485 C mol^{-1}) and n is the number of moles of the $Ni_xCo_yP_z$ (x=0.1, y=0.9, z=3) on the electrodes.

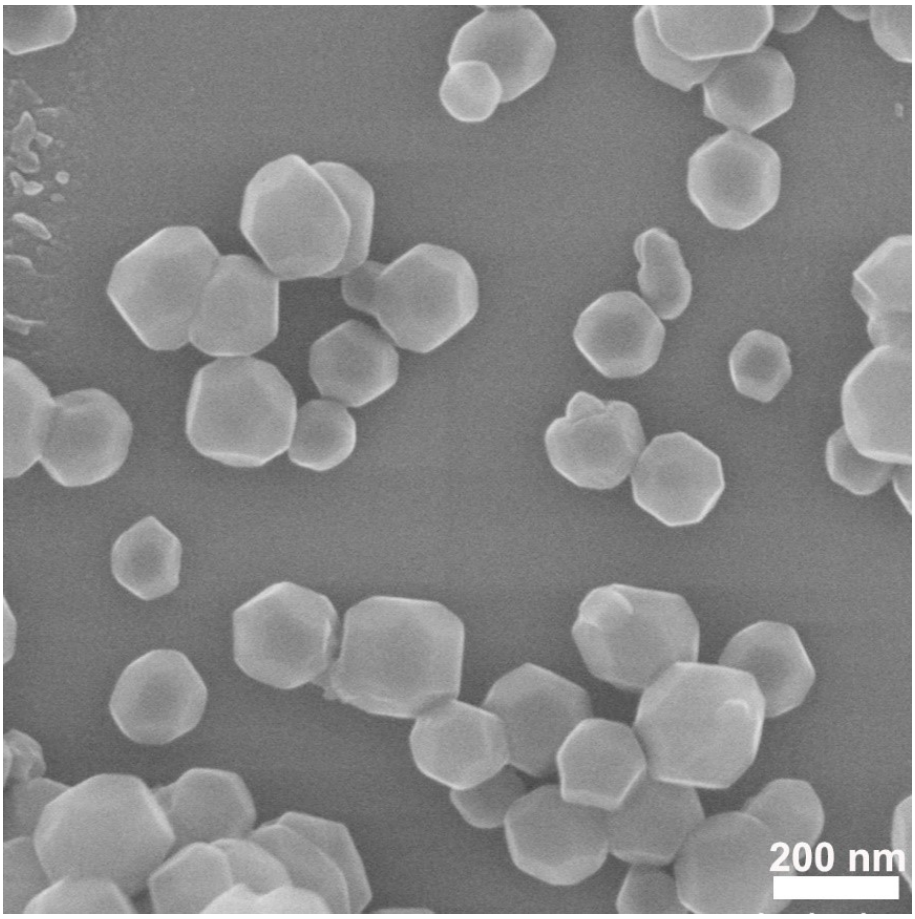

Figure S1. SEM image of Co-ZIF-67 polyhedron.

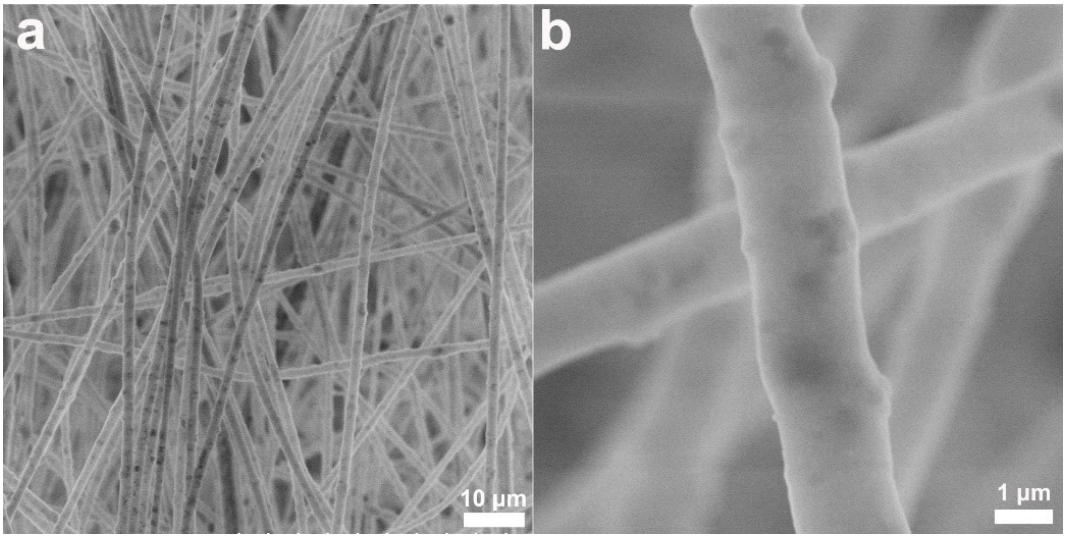

Figure S2. SEM images of ZIF-PAN fiber in the (a) large and (b) small scales.

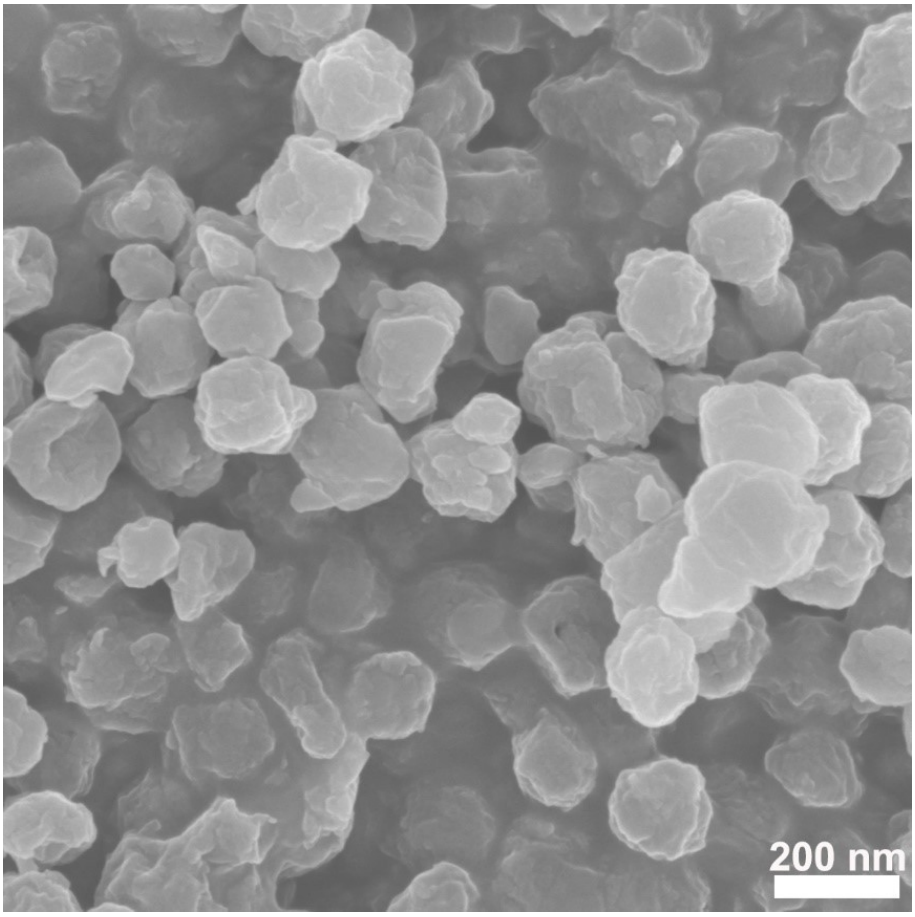

Figure S3. SEM image of CoP_x-CPHs.

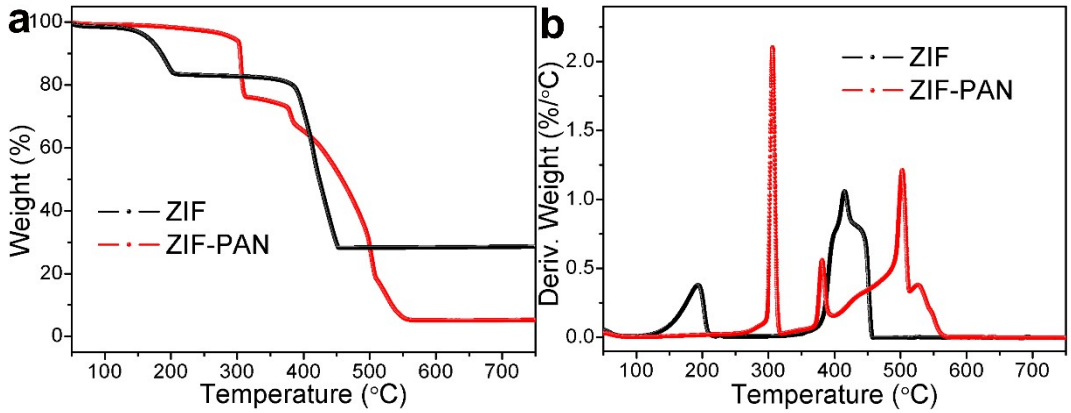

Figure S4. (a) TG and (b) DTG curves of ZIF and ZIF-PAN samples.

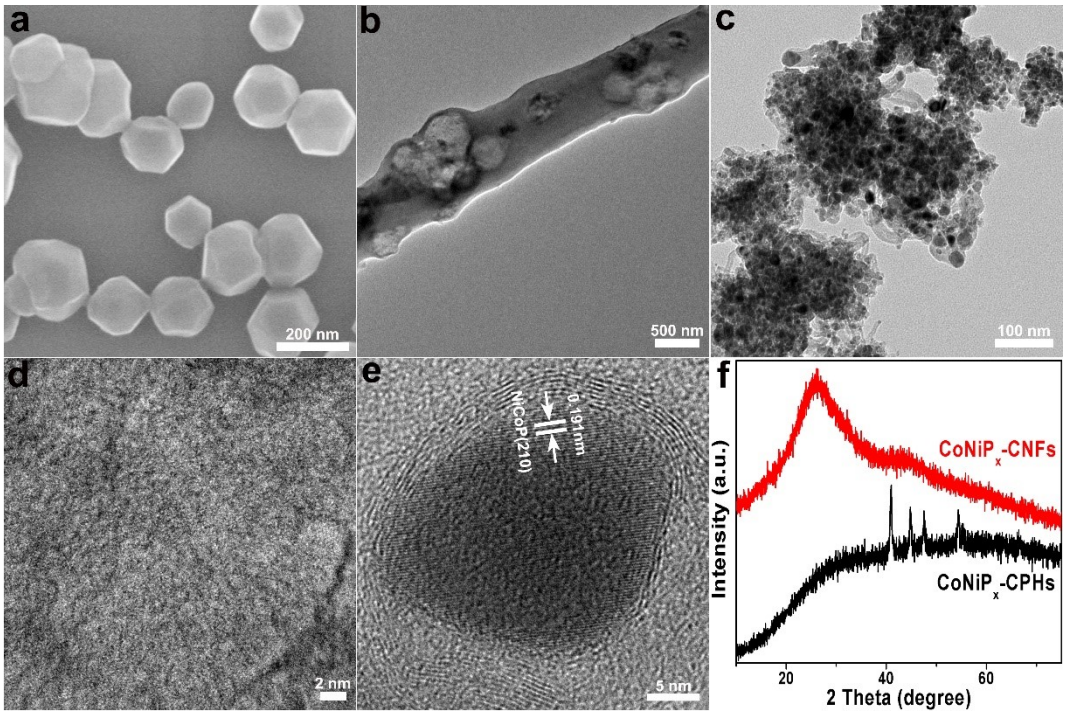

Figure S5. (a) SEM image of Ni-ZIF-67 polyhedron. TEM images of (b) $CoNiP_x$-CNFs and (c) $CoNiP_x$-CPHs. HRTEM images of (d) $CoNiP_x$-CNFs and (e) $CoNiP_x$-CPHs. (f) XRD patterns of $CoNiP_x$-CNFs and $CoNiP_x$-CPHs.

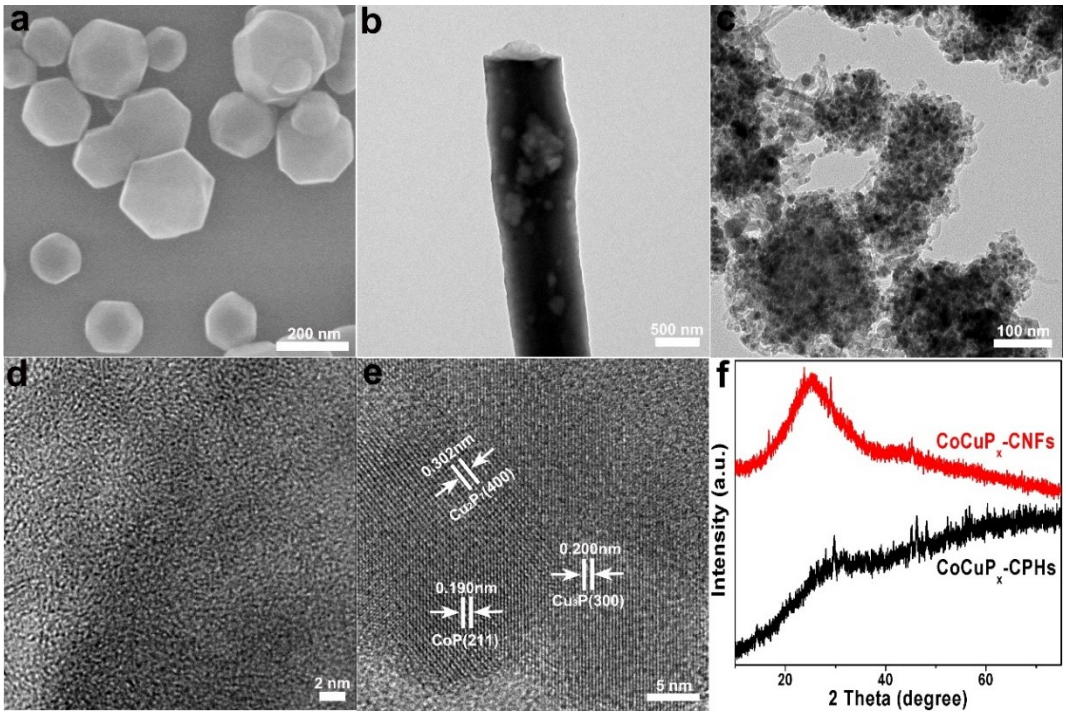

Figure S6. (a) SEM image of Cu-ZIF-67 polyhedron. TEM images of (b) $CoCuP_x$-CNFs and (c) $CoCuP_x$-CPHs. HRTEM images of (d) $CoCuP_x$-CNFs and (e) $CoCuP_x$-CPHs. (f) XRD patterns of $CoCuP_x$-CNFs and $CoCuP_x$-CPHs.

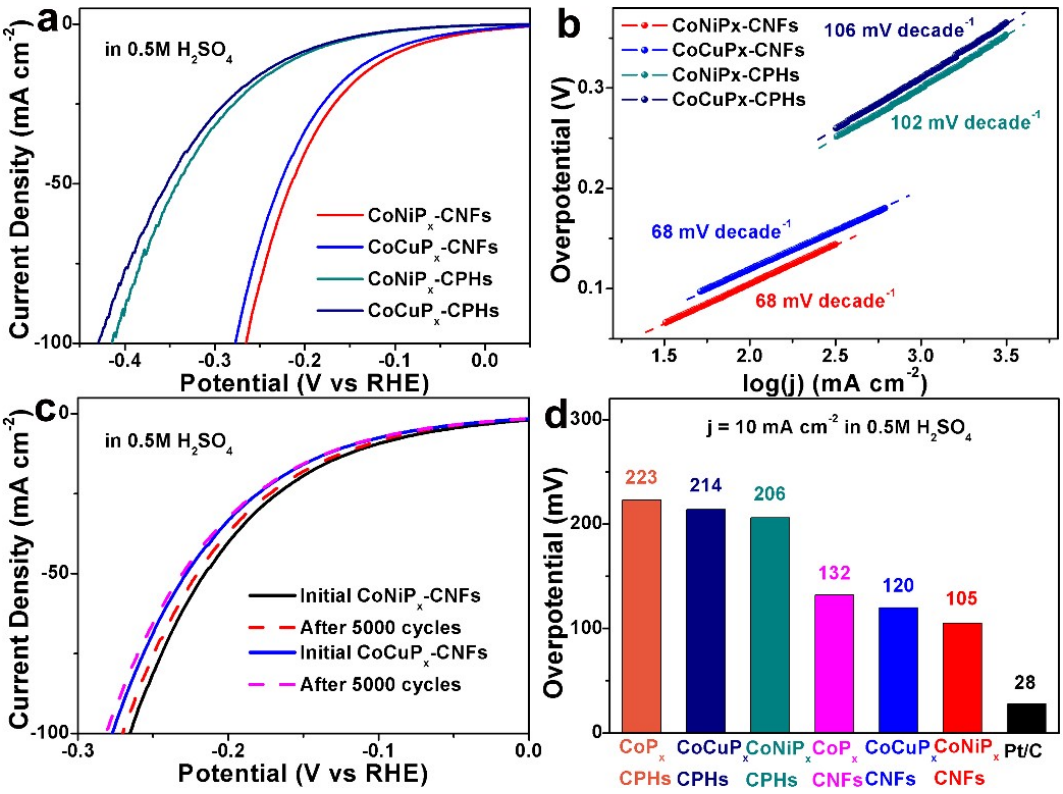

Figure S7. Electrochemical characterizations of $CoNiP_x$ and $CoCuP_x$ electrocatalysts for HER activity. (a) Polarization curves obtained in 0.5 M H_2SO_4 at 10 mV s^{-1} for $CoNiP_x$-CNFs, $CoNiP_x$-CPHs, $CoCuP_x$-CNFs and $CoCuP_x$-CPHs samples. (b) Tafel plots of the corresponding samples. (c) Polarization curves recorded in 0.5 M H_2SO_4 at 10 mV s^{-1} for $CoNiP_x$-CNFs and $CoCuP_x$-CNFs before and after 5000 cycles from 0.5 to -0.5 V vs RHE at 100 mV s^{-1} under acid condition. (d) The overpotential of the corresponding electrodes obtained at current density of 10 mA cm^{-2} in 0.5 M H_2SO_4.

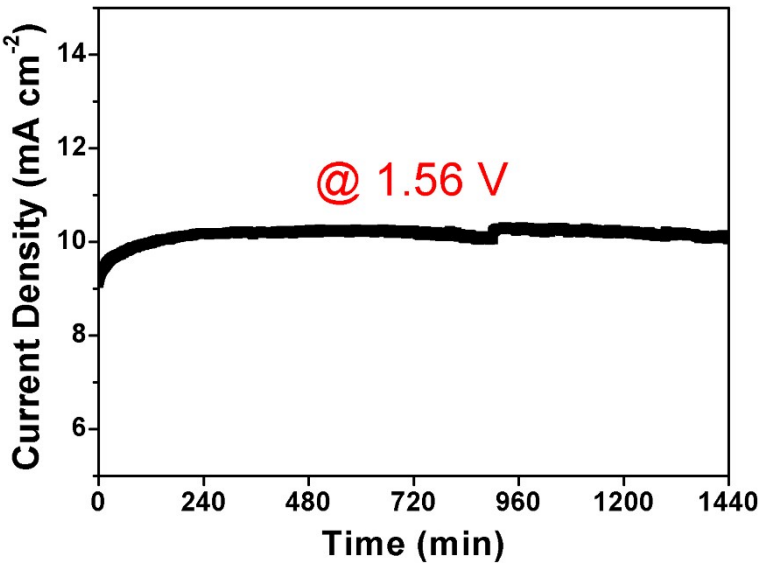

Figure S8. The time-dependent chronoamperometry test of $CoNiP_x$-CNFs electrocatalyst at applied potential of 1.56 V (vs. RHE) in 1.0 M KOH.

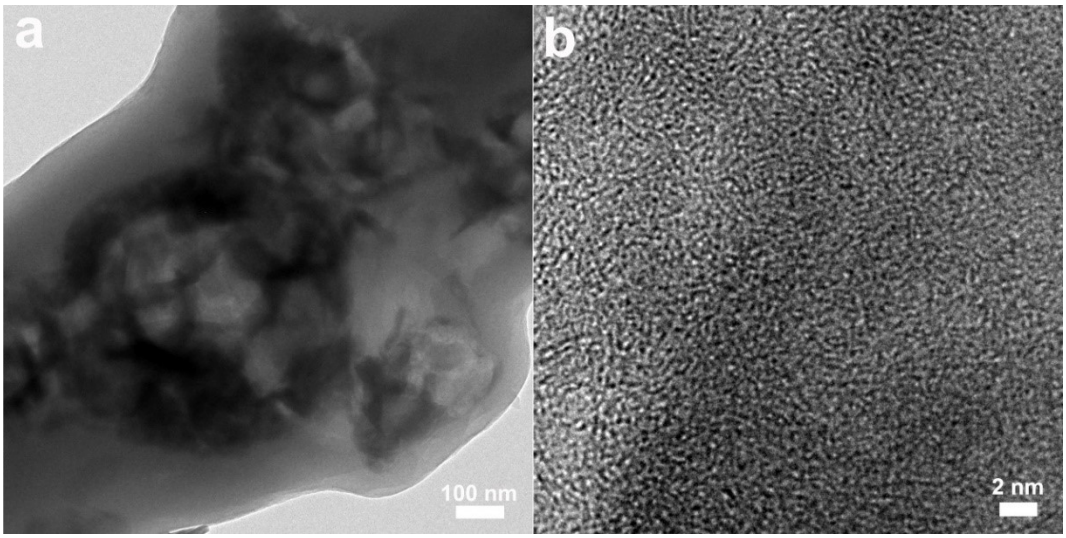

Figure S9. (a) TEM and (b) HRTEM images of $CoNiP_x$-CNFs electrocatalyst after 24 h chronoamperometry test.

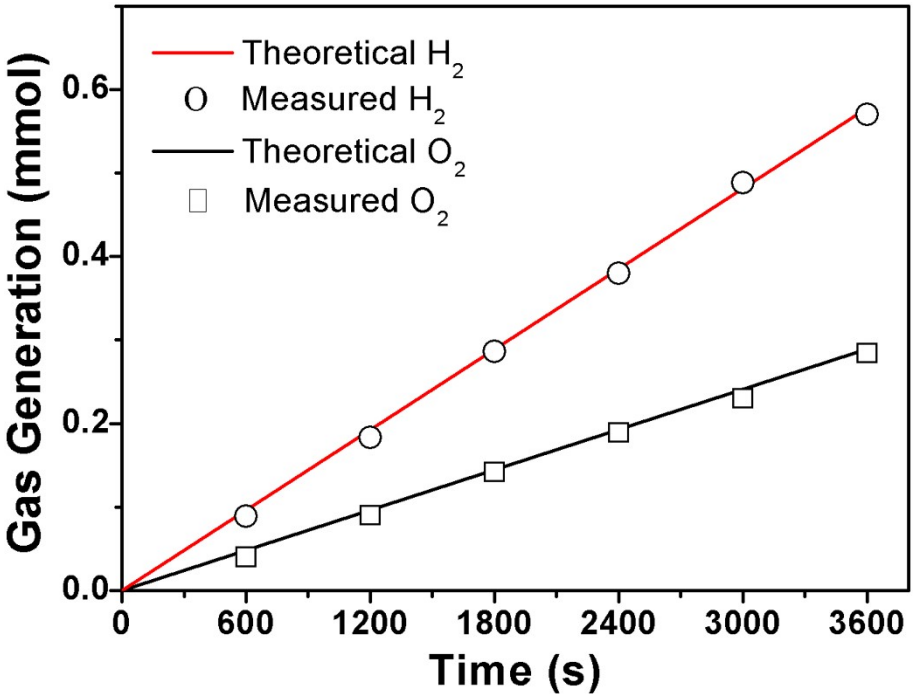

Figure S10. Faradaic efficiency of H_2 and O_2 production for overall water splitting.

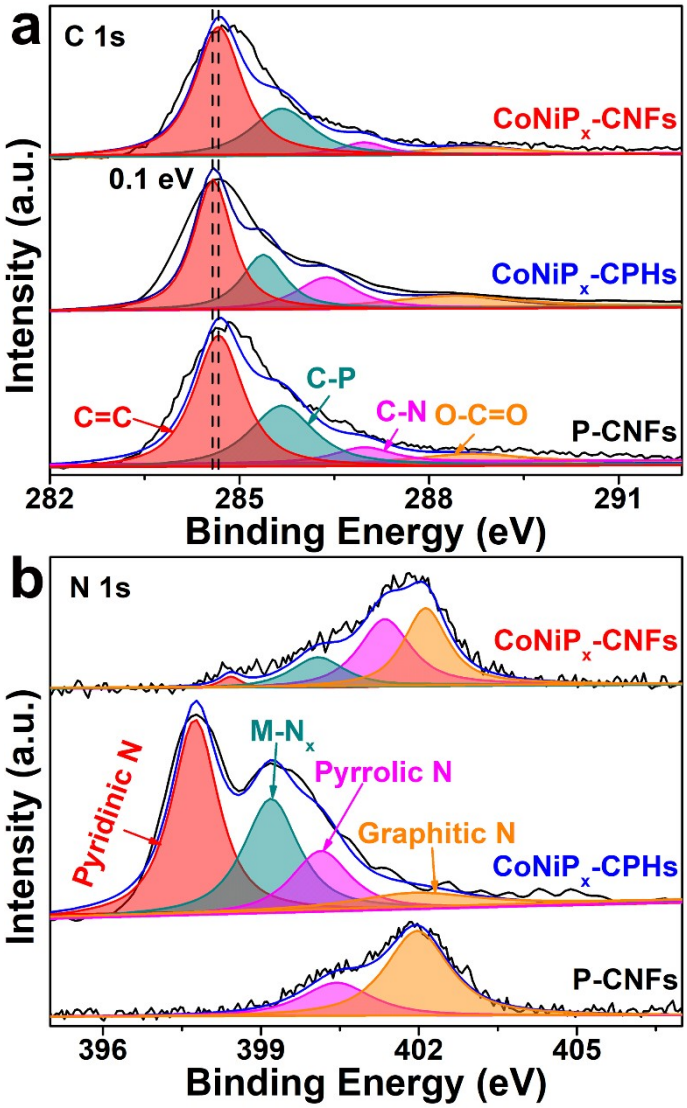

Figure S11. XPS spectra of (a) C 1s and (b) N 1s for P-CNFs, CoNiP$_x$-CNFs and CoNiP$_x$-CPHs.

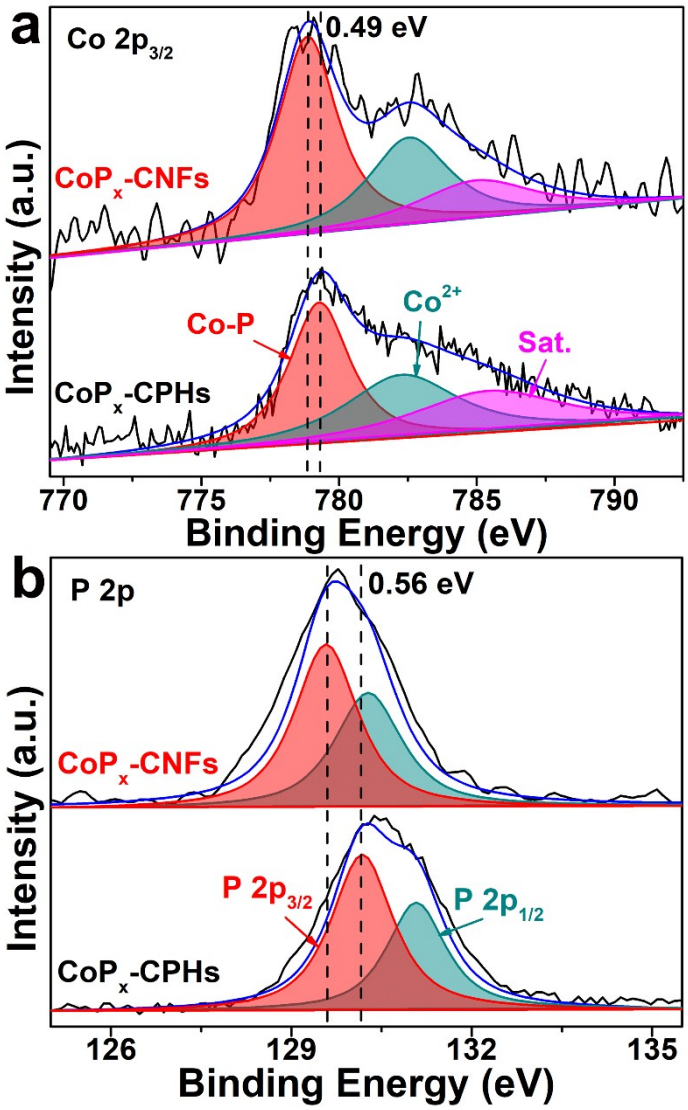

Figure S12. XPS spectra of (a) Co $2p_{3/2}$ and (c) P 2p for CoP_x-CNFs and CoP_x-CPHs.

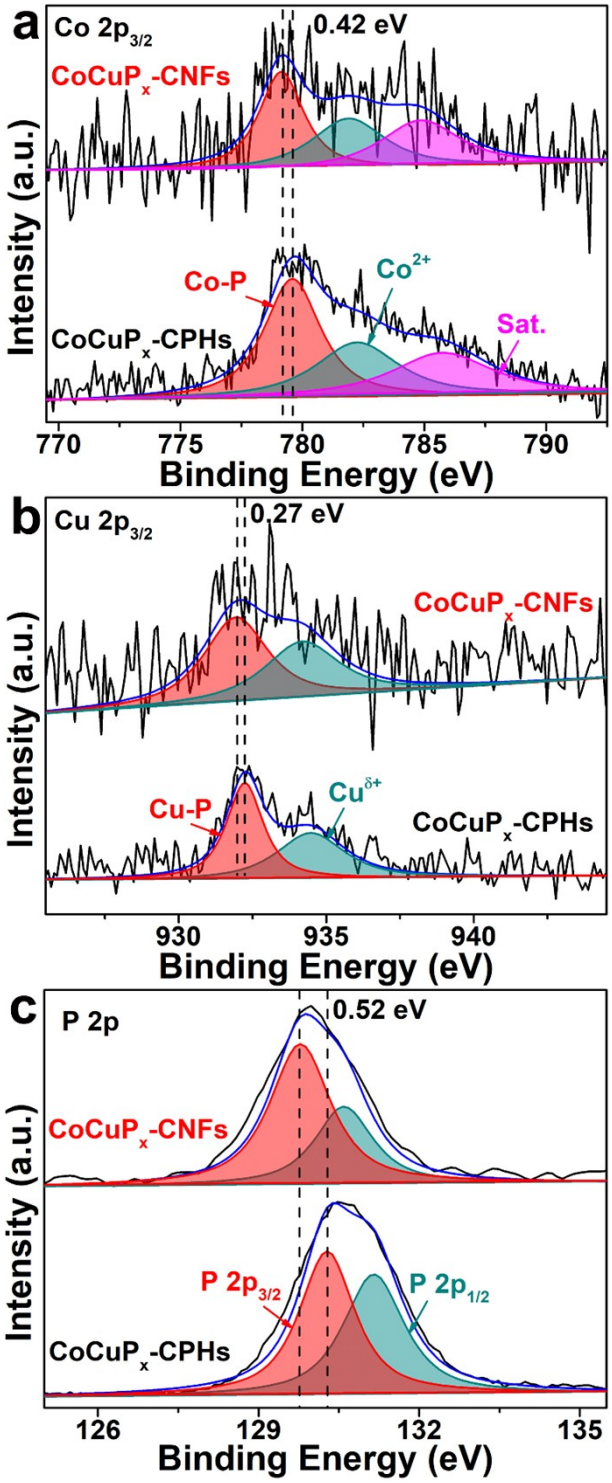

Figure S13. XPS spectra of (a) Co $2p_{3/2}$, (b) Cu $2p_{3/2}$ and (c) P 2p for $CoCuP_x$-CNFs and $CoCuP_x$-CPHs.

Table S1. The characteristic data of the Co-based phosphide samples

Samples	Element content (%)					
	Co [a]	Ni [a]	Cu [a]	P [b]	C [b]	N [b]
CoP_x-CNFs	2.47	0	0	4.52	62.31	11.85
$CoNiP_x$-CNFs	2.62	0.30	0	4.64	64.85	10.88
$CoCuP_x$-CNFs	2.57	0	0.24	4.57	65.18	11.26
CoP_x-CPHs	11.16	0	0	10.08	48.06	15.78
$CoNiP_x$-CPHs	10.89	1.75	0	9.34	48.55	14.65
$CoCuP_x$-CPHs	11.24	0	1.78	9.67	47.83	14.81

a Co, Ni and Cu loading amount in different samples were determined by the mass of Co, Ni and Cu element with ICP-MS analysis.

b P, C, and N content were measured by the X-ray photoelectron spectroscopy and CHN element analysis.

Table S2. The electrocatalytic performance comparison of the Co-based phosphide samples

Samples	**Overpotential to deliver 10 mA cm^{-2} (mV)**			**Impedance [a] (Ω)**
	HER in 0.5 M H_2SO_4	HER in 1.0 M KOH	OER in 1.0 M KOH	
CoP_x-CNFs	132	201	303	18.9
$CoNiP_x$-CNFs	105	154	269	18.8
$CoCuP_x$-CNFs	120	182	288	19.2
CoP_x-CPHs	223	290	365	98.3
$CoNiP_x$-CPHs	206	242	337	99.6
$CoCuP_x$-CPHs	214	276	345	99.2
P-CNFs	580	541	584	18.6

a The impedance was obtained via the fitting data using the ZView software.

Table S3. The surface area and pore structure comparison of the Co-based phosphide samples

Samples	BET surface area (m^2 g^{-1})	Pore diameter (nm)
CoP_x-CNFs	208.4	3.2
$CoNiP_x$-CNFs	215.7	3.0
$CoCuP_x$-CNFs	207.2	3.1
CoP_x-CPHs	238.6	3.5
$CoNiP_x$-CPHs	229.5	3.8
$CoCuP_x$-CPHs	244.8	3.3

Table S4. Comparison of HER performance of $CoNiP_x$-CNFs with those reported Co-based phosphide electrocatalysts in acid electrolytes

Catalysts	η_{10} (mV)	Mass loading	Substrate	Electrolytes	References
$CoNiP_x$-CNFs	105	0.5 mg cm^{-2}	GCE	0.5 M H_2SO_4	**This work**
$Ni_{0.67}Co_{1.33}P$/N-CNFs	100	0.287 mg cm^{-2}	GCE	0.5 M H_2SO_4	S1
$NiCo_2P_x$/CF	104	5.9 mg cm^{-2}	carbon felt	0.5 M H_2SO_4	S2
CoP-CNTs	139	0.27 mg cm^{-2}	GCE	0.5 M H_2SO_4	S3
CoP/Co_2P	99	0.36 mg cm^{-2}	GCE	0.5 M H_2SO_4	S4
CoP-400	113	0.43 mg cm^{-2}	GCE	0.5 M H_2SO_4	S5

Table S5. Comparison of HER performance of $CoNiP_x$-CNFs with those reported Co-based phosphide electrocatalysts in alkaline electrolytes

Catalysts	η_{10} (mV)	Mass loading	Substract	Electrolytes	References
$CoNiP_x$-CNFs	154	0.5 mg cm^{-2}	GCE	1.0 M KOH	**This work**
$Cu_{0.3}Co_{2.7}P$/NC	220	0.4 mg cm^{-2}	RDE	1.0 M KOH	S6
CoP-NW array	209	0.92 mg cm^{-2}	carbon cloth	1.0 M KOH	S7
Co_2P/CoNPC	208	0.39 mg cm^{-2}	GCE	1.0 M KOH	S8
Co_2P/CNT-900	132	0.75 mg cm^{-2}	GCE	1.0 M KOH	S9
$Co_{0.68}Fe_{0.32}P$	116	0.75 mg cm^{-2}	RRDE	1.0 M KOH	S10

Table S6. Comparison of OER performance of $CoNiP_x$-CNFs with those reported Co-based phosphide electrocatalysts in alkaline electrolytes

Catalysts	η_{10} (mV)	Mass loading	Substract	Electrolytes	References
$CoNiP_x$-CNFs	269	0.5 mg cm^{-2}	GCE	1.0 M KOH	**This work**
CoP/NCNHP	310	0.39 mg cm^{-2}	GCE	1.0 M KOH	S11
Co-P/NC	319	0.283 mg cm^{-2}	RDE	1.0 M KOH	S12
Fe_1Co_2-P/C	362	0.17 mg cm^{-2}	RDE	1.0 M KOH	S13
NiCoP/C	330	0.25 mg cm^{-2}	RDE	1.0 M KOH	S14
Co_2P/CoNPC	328	0.39 mg cm^{-2}	GCE	1.0 M KOH	S8

Table S7. Comparison of overall water splitting of $CoNiP_x$-CNFs with those reported Co-based phosphide electrocatalysts in alkaline electrolytes

Catalysts	η_{10} (V)	Mass loading	Substract	Electrolytes	References
$CoNiP_x$-CNFs	1.56	10 mg cm^{-2}	self-support	1.0 M KOH	**This work**
CoP/GO-400	1.70	0.28 mg cm^{-2}	RDE	1.0 M KOH	S15
Co_2P/CoNPC	1.64	0.39 mg cm^{-2}	GCE	1.0 M KOH	S8
Fe-CoP/Ti	1.60	1.03 mg cm^{-2}	Ti foil	1.0 M KOH	S16
$Ni_{0.67}Co_{1.33}P$/N-CNFs	1.56	0.287 mg cm^{-2}	GCE	1.0 M KOH	S1
Fe-CoP HTPAs	1.59	Not available	Ni foam	1.0 M KOH	S17

References

[S1] Q. Mo, W. Zhang, L. He, X. Yu, Q. Gao, ***Appl. Catal. B: Environ.***, 2019, 244, 620-627.

[S2] R. Zhang, X. Wang, S. Yu, T. Wen, X. Zhu, F. Yang, X. Sun, X. Wang, W. Hu, ***Adv. Mater.***, 2017, 29, 1605502.

[S3] C. Wu, Y. Yang, D. Dong, Y. Zhang, J. Li, ***Small***, 2017, 13, 1602873.

[S4] L. Chen, Y. Zhang, H. Wang, Y. Wang, D. Li, C. Duan, ***Nanoscale***, 2018, 10, 21019-21024.

[S5] H. Li, X. Zhao, H. Liu, S. Chen, X. Yang, C. Lv, H. Zhang, X. She, D. Yang, ***Small***, 2018, 14, 1802824.

[S6] J. Song, C. Zhu, B. Z. Xu, S. Fu, M. H. Engelhard, R. Ye, D. Du, S. P. Beckman, Y. Lin, ***Adv. Energy Mater.***, 2017, 7, 1601555.

[S7] J. Tian, Q. Liu, A. M. Asiri, X. Sun, ***J. Am. Chem. Soc.***, 2014, 136, 7587-7590.

[S8] H. Liu, J. Guan, S. Yang, Y. Yu, R. Shao, Z. Zhang, M. Dou, F. Wang, Q. Xu, ***Adv. Mater.***, 2020, 32, 2003649.

[S9] D. Das, K. K. Nanda, ***Nano Energy***, 2016, 30, 303-311.

[S10] F. Li, Y. Bu, Z. Lv, J. Mahmood, G.-F. Han, I. Ahmad, G. Kim, Q. Zhong, J.-B. Baek, ***Small***, 2017, 13, 1701167.

[S11] Y. Pan, K. Sun, S. Liu, X. Cao, K. Wu, W. C. Cheong, Z. Chen, Y. Wang, Y. Li, Y. Liu, D. Wang, Q. Peng, C. Chen, Y. Li, ***J. Am. Chem. Soc.***, 2018, 140, 2610-2618.

[S12] B. You, N. Jiang, M. Sheng, S. Gul, J. Yano, Y. Sun, ***Chem. Mater.***, 2015, 27, 7636-7642.

[S13] W. Hong, M. Kitta, Q. Xu, ***Small Methods***, 2018, 2, 1800214.

[S14] P. He, X. Y. Yu, X. W. Lou, ***Angew. Chem. Int. Ed.***, 2017, 56, 3897.

[S15] L. Jiao, Y. X. Zhou, H. L. Jiang, ***Chem. Sci.***, 2016, 7, 1690-1695.

[S16] C. Tang, R. Zhang, W. Lu, L. He, X. Jiang, A. M. Asiri, X. Sun, ***Adv. Mater.***, 2017, 29, 1602441.

[S17] E. Hu, J. Ning, D. Zhao, C. Xu, Y. Lin, Y. Zhong, Z. Zhang, Y. Wang, Y. Hu, ***Small***, 2018, 14, 1704233.